Journal of Molecular Structure 1038 (2013) 170–176

Contents lists available at SciVerse ScienceDirect

Journal of Molecular Structure

journal homepage: www.elsevier.com/locate/molstruc

FT-IR and FT-Raman spectroscopies and DFT calculations of 2,2-dimethyl-5-(4H-1,2,4-triazol-4-ylaminomethylene)-1,3-dioxane-4,6-dione monohydrate

G.M.M. Sampaio [a], A.M.R. Teixeira [a], H.D.M. Coutinho [a], D.M. de Sena Junior [a], P.T.C. Freire [b], P.E.S. Caselli [b], G.O.M. Gusmão [b], R.R.F. Bento [c,*], L.E. Silva [d]

[a] Universidade Regional do Cariri, 63010-970 Crato, Brazil
[b] Universidade Federal do Ceará, 60455-760 Fortaleza, Brazil
[c] Universidade Federal de Mato Grosso, 78060-900 Cuiabá, Brazil
[d] Universidade Federal do Paraná, Setor Litoral, Matinhos 83260-000, Brazil

HIGHLIGHTS

- ▶ We study the vibrational spectra of $C_9H_{10}N_4O_4{\cdot}H_2O$ molecule through Raman and infra red spectroscopies.
- ▶ We furnish the descriptions of the normal modes considering the Potential Energy Distribution (PED).
- ▶ We present calculated and theoretical data on geometric parameters of the molecule.
- ▶ We give detailed description of the assignments of the vibrational modes of $C_9H_{10}N_4O_4{\cdot}H_2O$.
- ▶ The first time the Potential Energy Distribution (PED) is being presented for this synthetic substance.

ARTICLE INFO

Article history:
Received 9 October 2012
Received in revised form 30 December 2012
Accepted 30 December 2012
Available online 11 January 2013

Keywords:
Raman scattering
IR spectroscopy
Normal modes
$C_9H_{10}N_4O_4{\cdot}H_2O$ crystal

ABSTRACT

In this work we present a study of the vibrational spectra of 2,2-dimethyl-5-(4H-1,2,4-triazol-4-ylaminomethylene)-1,3-dioxane-4,6-dione monohydrate, $C_9H_{10}N_4O_4{\cdot}H_2O$. The FT-IR and FT-Raman spectra of the crystal were recorded at room temperature in the regions 400–4000 cm^{-1} and 50–4000 cm^{-1}, respectively. Vibrational wavenumbers and wave vector were predicted using density functional theory calculations with the B3LYP functional and 6-31G(d,p) basis set. The descriptions of the normal modes were made after considering the Potential Energy Distribution (PED). A comparison with experimental spectra allowed us to assign all of the normal modes of the crystal.

1. Introduction

The synthesis of isolated pure substances has become a tool of great importance to the development of drugs with enhanced pharmacological properties. Nowadays, the use of molecular modeling contributes markedly to the discovery of new drugs, which are safer and more efficient. The compound 1,2,4-triazole and its derivatives have been used as starting materials for the synthesis of many heterocycles [1]. Studies indicate that the 1,2,4-triazole group is associated with anti-inflammatory action [2], and also with pharmacological activities, such as antiviral [3], analgesic [4], antimicrobial [5], antidepressant [6] and antifungal [7]. On the other hand, cyclic 1,3-diones like Meldrum's acid (2,2-dimethyl-1,3-dioxane-4,6-dione) and their 5-arylaminemethylene analogs play an important role in heterocyclic chemistry as pivotal intermediates to access cyclic products [8].

Derivatives of Meldrum's acid have proven to be valuable reagents and intermediates in the synthesis of complex organic compounds such as natural products and their analogs [9]. The search for a study to demonstrate the biological activity of 5-aminomethylene Meldrum's acid derivatives led to a patent in 1965 [10]. In addition, different heterocyclic rings were condensed to the 5-methoxymethylene Meldrum's acid in order to evaluate their potential biological activity as antileishmanicidal, antitrypanosomal and antiviral agent [8,11]. Furthermore, several compounds, natural or synthetic, can modify the antibiotic activity and also the phenotype of the bacterial strains, reversing the resistant and

* Corresponding author. Tel.: +55 65 3615 8743; fax: +55 65 3615 8734.
E-mail address: ricardobento@fisica.ufmt.br (R.R.F. Bento).

0022-2860/$ - see front matter © 2013 Elsevier B.V. All rights reserved.
http://dx.doi.org/10.1016/j.molstruc.2012.12.058

intermediary phenotype to the sensitive phenotype, as demonstrated by the derived compounds of 4-chloro-5-heteroimine-dithiazoles, against the *Escherichia coli*, *Staphylococcus aureus* and *Pseudomonas aeruginosa* strains [12].

Many heterocyclic derivatives of Meldrum's acid (2,2-dimethyl-1,3-dioxane-4,6-dione) have been prepared and studied from the synthetic and structural point of view [11], although their vibrational properties have not received the same attention. In order to fill this gap, the present work reports a study of vibrational spectra of 2,2-dimethyl-5-(4H-1,2,4-triazol-4-ylaminomethylene)-1,3-dioxane-4,6-dione monohydrate, $C_9H_{10}N_4O_4{\cdot}H_2O$, with support of theoretical calculations using density functional theory. As a consequence, we were able to assign the vibrational modes of the crystal this synthetic compound.

2. Experimental

The crystal structure of 2,2-dimethyl-5-(4H-1,2,4-triazol-4-ylaminomethylene)-1,3-dioxane-4,6-dione monohydrate, $C_9H_{10}N_4O_4{\cdot}H_2O$, an aminomethylene derivative of Meldrum's acid, was recently reported [13]. Crystalline samples of this compound were obtained after heating a solution of Meldrum's acid (36 mmol) in thimethyl orthoformate (50 mL) under reflux for 2 h, and adding the corresponding arylamine (30 mmol). Reflux was kept for additional 30 min. The material thus formed was filtered and washed with methanol.

FT-Raman spectrum, in the wavenumber region from 50 cm^{-1} to 4000 cm^{-1}, was taken using a Bruker RFS100/S FTR system and a liquid nitrogen cooled Ge D418-T detector, with a Nd:YAG laser emitting at 1064 nm as excitation source. Laser power was set to 150 mW, nominal resolution to 4 cm^{-1}, and accumulation of 60 scans per spectra. Slightly compacted powder samples were confined in screw cap standard chromatographic glass vials.

Infrared spectrum was obtained by using a Bruker Equinox/55 Fourier Transformed infrared (FT-IR) spectrometer equipped with a DTGS (deuterated triglycine sulfate) detector and a KBr beamsplitter. The wavenumber region covered in the mid-IR spectrum goes from 400 cm^{-1} to 4000 cm^{-1} with samples grinded in an agate mortar to minimize scattering on the particle surface, and mixed with KBr until a uniform mixture was obtained to form a pellet. The resolution was of 4 cm^{-1}. IR spectra were recorded and treated using spectroscopic software OPUS, from Bruker.

3. Computational method

The Density Functional Theory (DFT) algorithm was used in the calculation, and all the calculations in this work were performed by using Gaussian 03 software package [14]. The hybrid functional (B3LYP) and the basis set 6-31G, augmented by *d* polarization functions on heavy atoms and *p* polarization functions on hydrogen atoms, were used [15–17]. The initial molecular structure of $C_9H_{10}N_4O_4{\cdot}H_2O$ used in the DFT calculations corresponds to a single molecule of the unit cell described in Ref. [13]. The output file contained the optimized structure, the vibrational frequencies in the harmonic approximation, and the atomic displacements for each mode. The Potential Energy Distribution (PED) of the normal modes was calculated using the GAR2PED program [18]. The normal mode analysis was performed and the PED was calculated along the internal coordinates using localized symmetry [19,20]. For this purpose a complete set of 84 internal coordinates were defined using Pulay's recommendations [19]. The calculated vibrational wave numbers were adjusted to compare with experimental Raman and IR frequencies.

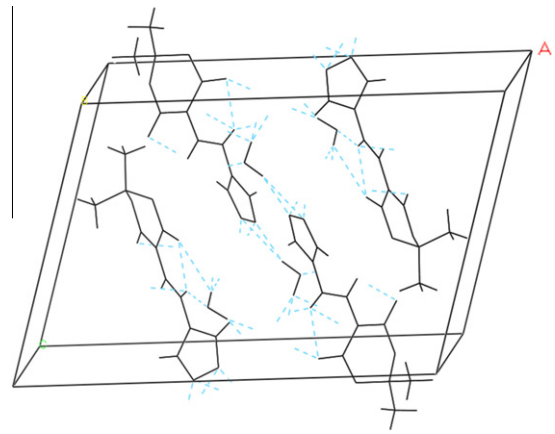

Fig. 2. Unit cell of $C_9H_{10}N_4O_4{\cdot}H_2O$ with dashed lines representing the hydrogen bonds.

4. Results and discussion

The molecular structure of 2,2-dimethyl-5-(4H-1,2,4-triazol-4-ylaminomethylene)-1,3-dioxane-4,6-dione monohydrate, $C_9H_{10}N_4O_4{\cdot}H_2O$ comprises two rings, named here as R1 and R2. R1 is a five-membered ring formed by atoms C1, C2, N1, N2 and N3 which comes from a 1,2,4 triazole group. R2, on its turn, is a six-membered ring formed by atoms C4 to C7, O2 and O3, originated from Meldrum's acid (2,2-dimethyl-1,3-dioxane-4,6-dione). The corresponding ball and stick model, with atom numbering, used to describe the $C_9H_{10}N_4O_4{\cdot}H_2O$ structure is shown in Fig. 1.

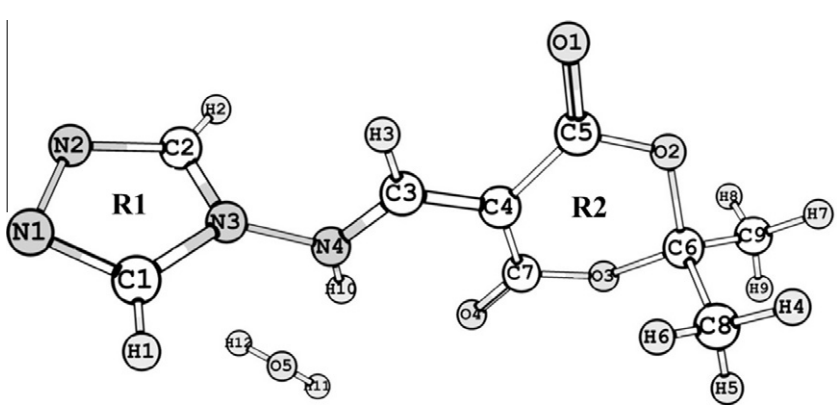

Fig. 1. Representation of the molecular structure of $C_9H_{10}N_4O_4{\cdot}H_2O$.

The crystal structure of $C_9H_{10}N_4O_4{\cdot}H_2O$ belongs to the monoclinic system, with space group $P2_1/c$, $Z = 4$, and lattice parameters: $a = 18.012$ Å, $b = 5.356$ Å, $c = 12.937$ Å, $\beta = 108.786°$ [13]. The distribution of the four molecules of $C_9H_{10}N_4O_4{\cdot}H_2O$ in the unit cell is shown in Fig. 2, where the dashed lines represent the hydrogen bonds among the molecules, which are responsible for the stabilization of the structure in the solid state, as occur with several other organic materials. The nitrogen atoms of ring R1 forms hydrogen bonds with one of the oxygen atoms of water molecule while the other oxygen form a hydrogen bond with the N4 atom of the $C_9H_{10}N_4O_4$ molecule. Additionally, some internal hydrogen bonds are formed, as those between the N4 atom and the oxygen of the ring R2.

It is well described in the literature that the biological activity, as well as the geometry of molecules, are influenced by internal hydrogen bonds. Furthermore, this issue is the subject of current

Table 1
Comparative tables of geometric parameters (calculated and experimental) of $C_9H_{10}N_4O_4{\cdot}H_2O$.

Bond lengths	Exp. (Å)	Calc. (Å)	Bond lengths	Exp. (Å)	Calc. (Å)
C1–N1	1.293	1.306	C5–O2	1.365	1.369
C1–N3	1.348	1.375	O2–C6	1.433	1.431
C1–H1	0.930	1.080	C6–O3	1.436	1.446
N1–N2	1.387	1.390	C6–C8	1.500	1.527
N2–C2	1.299	1.306	C6–C9	1.502	1.517
C2–N3	1.346	1.376	O3–C7	1.362	1.356
C2–H2	0.930	1.080	C7–O4	1.211	1.224
N3–N4	1.391	1.384	C8–H4	0.960	1.092
N4–C3	1.317	1.340	C8–H5	0.960	1.092
N4–H10	0.860	1.036	C8–H6	0.960	1.093
C3–C4	1.367	1.378	C9–H7	0.960	1.092
C3–H3	0.930	1.087	C9–H8	0.960	1.092
C4–C7	1.437	1.456	C9–H9	0.960	1.092
C4–C5	1.451	1.474	O5–H11	0.910	0.973
C5–O1	1.207	1.211	O5–H12	0.960	0.966
Bond angle	Exp. (°)	Calc. (°)	Bond angle	Exp. (°)	Calc. (°)
N1–C1–N3	109.7	110.0	O2–C6–O3	110.2	111.5
N1–C1–H1	125.1	127.1	O2–C6–C8	110.00	110.8
N3–C1–H1	125.1	122.9	O3–C6–C8	109.9	109.4
C1–N1–N2	107.6	107.6	O2–C6–C9	106.5	106.3
C2–N2–N1	106.6	107.6	O3–C6–C9	106.3	105.8
N2–C2–N3	110.1	110.0	C8–C6–C9	113.8	113.6
N2–C2–H2	124.9	127.1	C7–O3–C6	117.8	119.4
N3–C2–H2	124.9	122.9	O4–C7–O3	117.8	118.3
C2–N3–C1	105.9	104.9	O4–C7–C4	125.6	125.0
C2–N3–N4	127.0	127.5	O3–C7–C4	116.6	116.6
C1–N3–N4	127.0	127.4	C6–C8–H4	109.5	109.6
C3–N4–N3	119.5	119.2	C6–C8–H5	109.5	110.0
C3–N4–H10	125.8	126.2	H4–C8–H5	109.5	111.0
N3–N4–H10	114.7	114.6	C6–C8–H6	109.5	111.0
N4–C3–C4	126.4	128.5	H4–C8–H6	109.5	108.5
N4–C3–H3	116.8	115.1	H5–C8–H6	109.5	108.6
C4–C3–H3	116.8	116.4	C6–C9–H7	109.5	109.8
C3–C4–C7	121.8	123.4	C6–C9–H8	109.5	109.5
C3–C4–C5	117.2	115.8	H7–C9–H8	109.5	109.1
C7–C4–C5	120.8	120.5	C6–C9–H9	109.5	110.0
O1–C5–O2	117.9	119.4	H7–C9–H9	109.5	109.3
O1–C5–C4	126.3	125.3	H8–C9–H9	109.5	109.2
O2–C5–C4	115.8	115.3	H11–O5–H12	107.0	104.7
C5–O2–C6	118.3	119.5			
Torsion angle	Exp. (°)	Calc. (°)	Torsion angle	Exp. (°)	Calc. (°)
N3–C1–N1–N2	0.6	0.4	C7–C4–C5–O2	−5.4 (3)	−7.1
C1–N1–N2–C2	0.1	0.2	O1–C5–O2–C6	159.2 (2)	161.2
N1–N2–C2–N3	−0.8	−0.7	C4–C5–O2–C6	−23.0 (3)	−21.5
N2–C2–N3–C1	1.1	0.9	C5–O2–C6–O3	49.5 (2)	46.2
N2–C2–N3–N4	176.18	176.3	C5–O2–C6–C8	−71.8 (2)	−75.4
N1–C1–N3–C2	−1.1	−0.8	C5–O2–C6–C9	164.38 (18)	161.1
N1–C1–N3–N4	−176.12	−176.2	O2–C6–O3–C7	−49.7 (2)	−44.2
C2–N3–N4–C3	77.5	86.9	C8–C6–O3–C7	71.7 (2)	78.0
C1–N3–N4–C3	−108.4	−98.7	C9–C6–O3–C7	−164.71 (18)	−159.3
N3–N4–C3–C4	−177.2	−178.8	C6–O3–C7–O4	−159.60 (18)	−164.8
N4–C3–C4–C7	2.8	2.7	C6–O3–C7–C4	23.6 (3)	17.7
N4–C3–C4–C5	177.6	177.0	C3–C4–C7–O4	3.1 (3)	5.6
C3–C4–C5–O1	−2.6	−4.5	C5–C4–C7–O4	−171.5 (2)	−168.5
C7–C4–C5–O1	172.2	170.0	C3–C4–C7–O3	179.60 (18)	177.2
C3–C4–C5–O2	179.8	178.5	C5–C4–C7–O3	5.0 (3)	8.8

Hydrogen-bond geometry (Å, °)

D–H···A	D–H		H···A		D···A		D–H···A	
	Exp.	Calc.	Exp.	Calc.	Exp.	Calc.	Exp.	Calc.
N4–H10···O4	0.9	1.0	2.2	2.3	2.8	2.9	119.6	112.3
N4–H10···O5	0.9	1.0	2.0	1.8	2.7	2.8	142.0	164.8

research in chemistry, due to the influence of these interactions in the design of new biologically active substances, affecting membrane transport and the distribution of drugs within biological system. In general terms the formation of ligand–protein complexes depends on hydrogen bonding. As it is well known, hydrogen bond contributes to the orientation of the ligand associated by a conformational distortion of the molecules and recognition of substrates, inhibitors, agonists and antagonists, among others [21–25].

The molecule $C_9H_{10}N_4O_4{\cdot}H_2O$ has 30 atoms, and so there are 90° of freedom. Excluding the translational and rotational modes, there are 84 vibrational modes for the hydrate. In the unit cell there are four units of the hydrate $C_9H_{10}N_4O_4{\cdot}H_2O$, accounting for 360° of freedom and thus 354 vibrational modes are expected. From these, three are acoustic modes and 351 are optical modes. The modes of A_g and B_g irreducible representations of the factor group C_{2h} are Raman active, while modes with A_u and B_u symmetries are infrared active. Assuming that the weakness of the intermolecular coupling causes negligible factor group splitting, the assignment task is simplified to that of the molecular modes.

Table 1 shows bond distances, bond angles and dihedral angles for the hydrate $C_9H_{10}N_4O_4{\cdot}H_2O$, for the optimized structure (Calc.) and that obtained from X-ray analysis (Exp.) [13]. The agreement between the optimized and experimental crystal structure is quite good, showing that the geometry optimization reproduces the experimental conformation almost exactly.

The FT-Raman and FT-IR spectra of polycrystalline samples of the substance $C_9H_{10}N_4O_4{\cdot}H_2O$ are shown in Figs. 3a and b, respectively. From the FT-Raman spectrum we observe that modes below 200 cm^{-1} – some of them associated to external modes and others to internal modes as discussion below – are the most intense in all spectral range, at least from 0 to 1750 cm^{-1} interval.

Table 2 lists a detailed description of the assignments of the vibrational modes of $C_9H_{10}N_4O_4{\cdot}H_2O$. The calculated wavenumber values, not scaled, are given in the first column, while the calculated and scaled wavenumbers – whose meaning will be furnished below – are given in the second column. We also present the experimental wavenumber values for the crystal obtained by FT-Raman and FT-IR spectroscopies (the third and fourth columns, respectively); and the fifth column gives the assignment of the all bands appearing in both Raman and infra red spectra. The vibrational assignments of the normal modes were made with regard to the PED, where values greater than 10% only are considered. The percent contribution of the PED to each vibrational mode is given in parentheses in the fourth column.

The symbols employed in the classification of the normal modes are as follows: r, τ, sc and wag stand for rocking, torsion, scissoring and wagging vibrations, respectively. The symbol δ is used to indicate a bending and when associated with the subscript 'out' refers to an out-of-plane deformation. Finally, ν_s and ν_{as} are used to indicate symmetric and anti-symmetric stretching, respectively. With regard to the intensity of the Raman and of the infrared bands we have used the following abbreviations: vs (very strong), s (strong), m (medium), w (weak) and vw (very weak).

Now we discuss the main calculated and observed vibrations of $C_9H_{10}N_4O_4{\cdot}H_2O$. The calculated values for the wavenumbers at the DFT level contain known systematic errors due to the neglect of electron correlation, resulting in overestimates of about 10–20%. Therefore, it is necessary to calculate a suitable scale factor (f) to achieve a better agreement with the experimental values. Following the procedure described by Wong [26] and Scott and Radom [27], f was calculated by fitting the theoretical values to the experimental ones (from FT-Raman spectrum). After successive adjustments, f was found to be 0.9495 with the overall root mean square error for this scale factor of 56 cm^{-1}. In Table 2, the scaled wavenumbers (ω_{scal}) were obtained by multiplying the calculated values (ω_{cal}) by f. The assignments of the respective molecular vibrations are given in the last column.

Analysis of the normal modes from the crystal shows that most of the bands in the FT-Raman and FT-IR spectra consist of combined vibrational modes. The out of plane deformation are mainly present in the region between 30 $cm^{-1} \leqslant \omega_{cal} \leqslant 900$ cm^{-1}, but can also be observed until $\omega_{cal} = 1332$ cm^{-1}. The torsional modes are observed in the region of calculated frequencies between 104 cm^{-1} and 684 cm^{-1}. However, vibrations related to the methyl

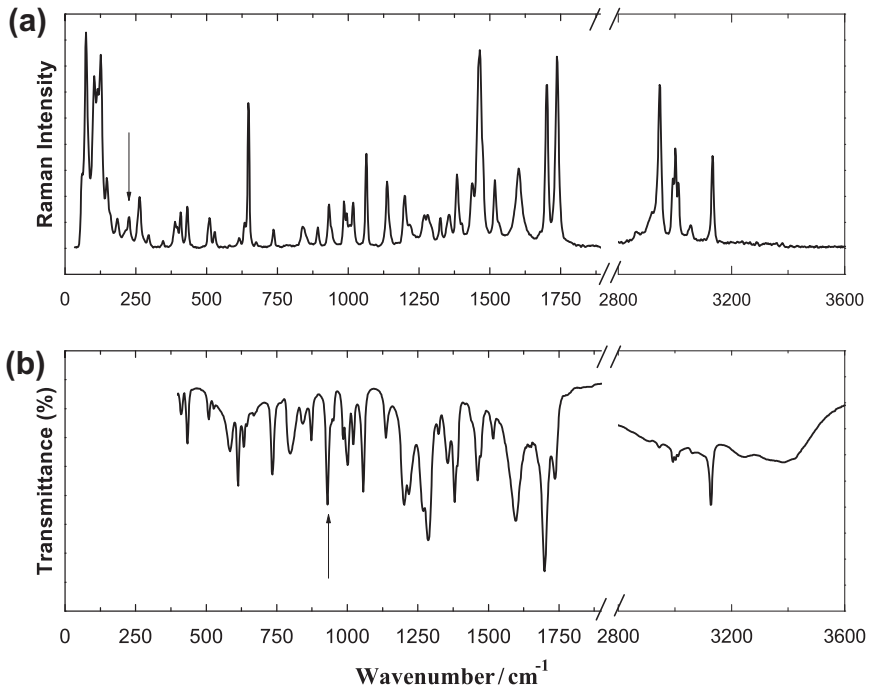

Fig. 3. Vibrational spectra of $C_9H_{10}N_4O_4{\cdot}H_2O$ crystal at room temperature: (a) FT-Raman and (b) FT-IR. The vertical arrows in (a), at 207 cm^{-1}, and (b), at 930 cm^{-1}, are associated with the atomic displacements in Fig. 4a and b, respectively.

Table 2
Calculated vibrational wavenumbers (in cm^{-1}), scaled values for $f = 0.9495$, experimental Raman and IR bands positions in units of cm^{-1}, and assignment of vibrational modes.

ω_{calc}	ω_{scal}	$\omega_{FT\text{-}Raman}$	$\omega_{FT\text{-}IR}$	Assignment with PED[a] (%)
30	28			δ_{out} (C7C4C3C5) (73) + δ_{out} (C3N4HN3) (18)
35	33			δ_{out} (C3N4HN3) (89)
39	37			δ_{out} (C3N4HN3) (79) + δ_{out} (C7C4C3C5) (14)
52	49	61 m		δ_{out} (C2N3N4C1) (72)
78	74	74 vs		δ_{out} (C3N4HN3) (90)
104	99	104 vs		R2[τ (C4C5O2C6)] (95)
121	115	115 vs		R2[δ (C7C4C5;O2O3C6)] (32) + δ_{out} (C2N3N4C1) (27) + δ_{out} (C7C4C3C5) (18)
130	123	125 vs		δ_{out} (C7C4C3C5) (42) + R2[τ (C4C5O2C6)] (18) + R2[δ (C4O2C5;O3C4C7)] (13)
160	152	148 m		R2[τ (C4C5O2C6)] (20) + δ_{out} (C3N4HN3) (20) + δ_{out} (C2N3N4C1) (13) + R2[δ (C4O2C5;O3C4C7)] (13)
201	191	161 m		δ_{out} (C7C4C3C5) (65) + δ_{out} (C2N3N4C1) (15)
217	206	185 m		δ_{out} (C7C4C3C5) (84) + δ_{out} (C3N4HN3) (11)
220	209	207 w		R2[τ ($C8H_3$;$C9H_3$)] (79) + δ_{out} (C7C4C3C5) (16)
250	237	214 w		R2[δ (C7C4C5;O2O3C6)] (70) + δ_{out} (C2N3N4C1) (13)
258	245	226 m		R2[τ ($C8H_3$; $C9H_3$)] (33) + R2[δ (C4O2C5;O3C4C7)] (21) + δ_{out} (C3N4HN3) (17)
259	246	263 m		R2[τ ($C8H_3$;$C9H_3$)] (42) + δ (HO5H) (29) + δ_{out} (C3N4HN3) (13)
296	281	295 w		R2[τ (C4C5O2C6)] (41) + R2[δ (C4O2C5;C6C7O3)] (26) + R2[τ ($C8H_3$;$C9H_3$)] (26)
335	318	317 vw		δ_{out} (C7C4C3C5) (24) + R2[δ (C4O2C5;O3C4C7)] (17) + δ (HN4N3) (16)
343	326	328 vw		δ_{out} (C7C4C3C5) (59) + δ_{out} (C3N4HN3) (35)
387	367	346 w		R2[τ (C4C5O2C6)] (60) + δ_{out} (C3N4HN3) (17) + δ (C6C8H) (11)
401	381	360 vw		δ_{out} (C7C4C3C5) (51) + δ_{out} (C3N4HN3) (28)
419	398	389 m		δ_{out} (C7C4C3C5) (58) + δ_{out} (C3N4HN3) (15) + δ_{out} (C4C3HN4) (14)
422	401	396 m		δ_{out} (C3N4HN3) (81)
433	411	408 m	412 m	δ_{out} (C7C4C3C5) (61) + δ_{out} (C3N4HN3) (22) + δ_{out} (C4C3HN4) (11)
505	479	432 m	434 s	R2[δ (C4O2C5;C6C7O3)] (49) + R2[δ (C4O2C5;O3C4C7)] (26) + δ_{out} (C7C4C3C5) (11)
509	483	447 vw		R2[δ (C7C4C5;O2O3C6)] (95)
525	498	487 vw		R2[δ (C7C4C5;O2O3C6)] (78) + δ_{out} (C7C4C3C5) (17)
588	558	510 m	509 m	R1[τ (N2N1C1N3)] (43) + δ (HN4N3) (30) + δ_{out} (C2N3N4C1) (13)
625	593	529 m	528 w	R1[τ (N2N1C1N3)] (54) + δ_{out} (C2N3N4C1) (20)
638	606	550 vw		R1[τ (N2N1C1N3)] (44) + δ_{out} (C2N3N4C1) (26)
644	611	564 vw		δ_{out} (C7C4C3C5) (49) + R2[δ (C7C4C5;O2O3C6)] (23)
684	649	581vw	584 s	R1[τ (N2N1C1N3)] (57)+R1[δ_{out} (N3C1HN1)] (24)
721	685	615 w	613 s	δ_{out} (C4C3HN4) (63) + R2[τ (C4C5O2C6)] (22) + δ_{out} (C3N4HN3) (13)
741	704	634 m	634 m	δ_{out} (C7C4C3C5) (46) + R2[δ (C7C4C5;O2O3C6)] (31)
784	744	648 s	644 m	δ_{out} (C7C4C3C5) (92)
806	765	675 w	669 w	R1[δ_{out} (N3C1HN1)] (73) + R1[δ_{out} (N2C2HN3)] (25)
833	791	736 m	735 s	R1[δ_{out} (N3C1HN1)] (74) + R1[δ_{out} (N2C2HN3)] (21)
849	806	840 m	798 s	R1[δ_{out} (N3C1HN1)] (46) + R1[δ_{out} (N2C2HN3)] (11)
871	827	856 w	843 m	δ_{out} (C3N4HN3) (65) + δ_{out} (C4C3HN4) (23)
900	855	892 m	873 m	δ_{out} (C7C4C3C5) (31) + R2[δ (C7C4C5;O2O3C6)] (23)+ δ_{out} (C3N4HN3) (18) + R2[δ (C7C4C5;O2O3C6)] (13)
935	888	932 m	930 s	R1[δ (C1N3C2N2N1)] (83)
945	897	941 m	951 m	r ($C8H_3$) (30) + R2[δ (C7C4C5;O2O3C6)] (15) + δ ($C9H_3$) (12)
952	904	985 m	985 m	R2[δ (C7C4C5;O2O3C6)] (24) + R2[δ (C4O2C5;C6C7O3)] (22)
1001	950	994 m		R1[δ (C2N2N3)] (37) + R1[δ (C1N1N3)] (17) + R1[ν (N1N2)] (15)
1014	963	1006 m	1001s	δ_{out} (C4C3HN4) (51) + R2[δ (C7C4C5;O2O3C6)] (27) + δ_{out} (C7C4C3C5) (11)
1024	972	1017 m	1021 m	r ($C8H_3$) (53) + r ($C9H_3$) (22)
1041	988	1063 m	1057 s	δ_{out} (C4C3HN4) (87)
1048	995	1097 vw		δ_{out} (C4C3HN4) (80)
1070	1016	1137 m	1136 m	R1[δ (C2N2N3)] (43) + R1[δ (C1N3C2N2N1)] (20) + R1[ν (C1N3)] (12) + R1[δ (C1N1N3)] (11)
1156	1098	1168 vw		δ (HN4N3) (16) + R1[δ (C1N1N3)] (16) + δ (N4C3C4) (16)
1222	1160	1200 m	1202 w	R1[δ (C1N1N3)] (89)
1224	1162	1218 m	1218 s	R1[δ (C2N2N3)] (62) + R1[δ (C1N1N3)] (25)
1235	1173	1234 vw		R2[δ (C7C4C5;O2O3C6)] (83)
1255	1192	1243 vw		R2[δ (C7C4C5;O2O3C6)] (23) + R2[δ (C4C5C7)] (20) + R1[δ (C1N1N3)] (12)
1290	1225	1269 m	1268 s	δ (N4C3C4) (22) + R2[δ (C7C4C5;O2O3C6)] (22) + δ (HN4N3) (12)
1301	1235	1280 m	1287 vs	R2[δ (C7C4C5;O2O3C6)] (57) + δ (N4C3C4) (32)
1332	1265	1295 m		δ_{out} (C3N4HN3) (35) + R1[ν (C1N3)] (24) + R1[δ (C1N3C2N2N1)] (19)
1341	1273	1325 m	1323 w	δ (N4C3C4) (46) + R2[δ (C7C4C5;O2O3C6)] (23) + δ (HN4N3) (23)
1405	1334	1356 m	1355 m	δ (HN4N3) (38) + R2[δ (C7C4C5;O2O3C6)] (24) + δ (N4C3C4) (16)
1420	1348	1384 m	1380 s	wag ($C9H_3$) (69) + wag ($C8H_3$ (25)
1435	1363	1401w	1390 m	δ (HN4N3) (54) + wag ($C8H_3$) (18)
1439	1366	1438 m	1437 w	δ (HN4N3) (78)
1491	1416	1463 vs	1462 m	sc ($C9H_3$) (74) + sc ($C8H_3$) (14)
1492	1417			sc ($C9H_3$) (49) + sc ($C8H_3$) (16) + δ (HN4N3) (14)
1508	1432	1474 m	1472 m	δ (HN4N3) (72)
1510	1434			δ (HN4N3) (64) + R2[δ (C7C4C5;O2O3C6)] (21)
1514	1438	1517 m	1517 w	sc ($C9H_3$) (52) + δ (HN4N3) (15)
1518	1441	1533 w	1539 vw	δ (HN4N3) (51) + R1[δ (C2N2N3)] (23)
1545	1467	1602 m	1597 s	δ (HN4N3) (34) + R1[δ (C1N1N3)] (24) + R1[δ (C2N2N3)] (20)
1656	1572	1643 vw	1645 vw	δ (HN4N3) (53) + **δ** (HO5H) (33)
1681	1596	1678 vw	1675 m	δ (HN4N3) (50) + **δ** (HO5H) (42)
1776	1686	1701vs	1699 vs	R2[ν (C7O4)] (61) + R2[δ (C7C4C5;O2O3C6)] (15) + R2[δ (C4O2C5;C6C7O3)] (12)
1833	1740	1737 vs	1736 s	R2[δ (C7C4C5;O2O3C6)] (76)
3066	2911	2749 w		ν_s ($C8H_3$) (92)
3075	2920	2863 w		ν_s ($C9H_3$) (88)

Table 2 (*continued*)

ω_{calc}	ω_{scal}	$\omega_{FT\text{-}Raman}$	$\omega_{FT\text{-}IR}$	Assignment with PED[a] (%)
3145	2986	2886 vw		ν_{as} (C8H$_3$) (97)
3153	2994	2920 m	2912 w	ν_{as} (C8H$_3$) (56) + ν_{as} (C9H$_3$) (27) + δ (C6C8H) (12)
3161	3001	2947 vs	2944 w	ν_{as} (C9H$_3$) (82)
3162	3002	2993 m	2992 m	ν_{as} (C9H$_3$) (93)
3197	3036	3002 s	3003 m	ν (N4H) (86) +
3211	3049	3012 s	3013 m	ν (C3H) (59) + δ(N4H) (32)
3283	3117	3056 w	3060 w	R1[ν (C2H)] (80) + R1[ν (C1H)] (15)
3288	3122	3133 s	3127 s	R1[ν (C1H)] (89)
3721	3533		3241 m	ν_s (HO5H) (82)
3872	3676		3385 m	ν_{as} (HO5H) (97)

Nomenclature: τ = torsion; sc = scissoring; δ = bending; δ_{out} = out of plane bending; ν = stretching; ν_{as} = asymmetric stretching; ν_s = symmetric stretching. vs = very strong; s = strong; m = medium; w = weak; vw = very weak.

[a] Only PED values greater that 10% are given.

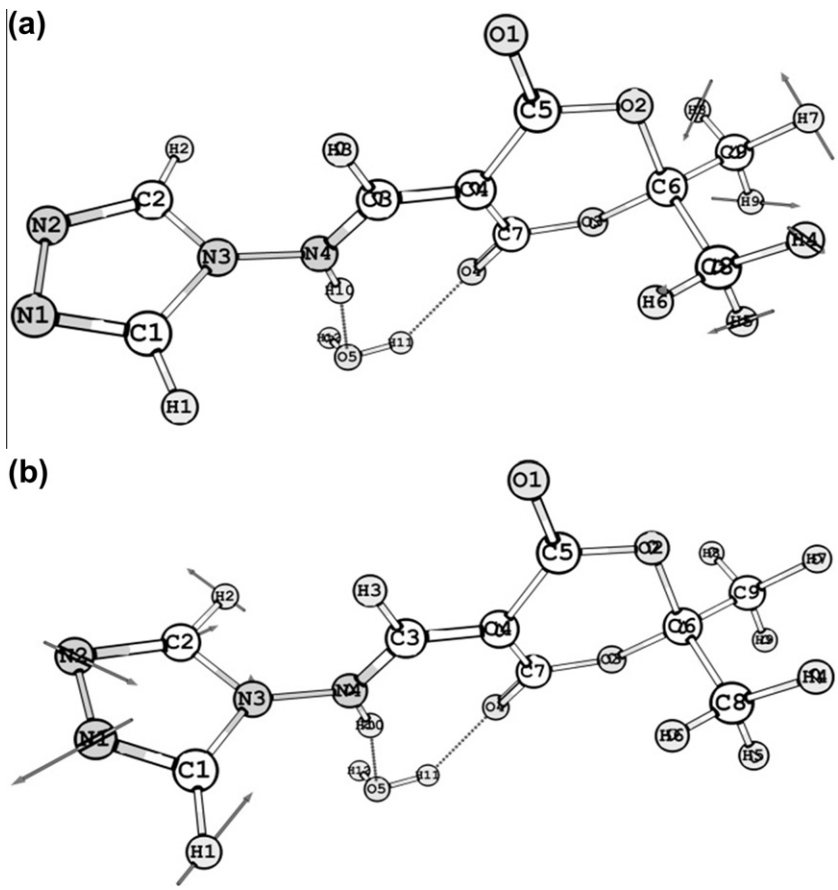

Fig. 4. Selected representations of atomic vibrations corresponding to the calculated wavenumbers of $C_9H_{10}N_4O_4{\cdot}H_2O$: (a) ω_{cal} = 220 cm^{-1} and (b) ω_{cal} = 935 cm^{-1}.

groups were clearly observed at the usual wavenumbers such as: torsion of CH_3 in ω_{cal} = 258 cm^{-1} and ω_{cal} = 259 cm^{-1}, rocking of CH_3 in ω_{cal} = 1024 cm^{-1}, wagging of CH_3 in ω_{cal} = 1420 cm^{-1} and ω_{cal} = 1435 cm^{-1}, and scissoring of CH_3 in ω_{cal} = 1491 cm^{-1}. The two very intense bands observed above 1700 cm^{-1} are assigned as vibrations of R2 ring, both stretching of C7O4 and bending of C7C4C5;O2O3C6 group.

For organic crystals, bands resulting from C–H, CH_2, CH_3, and N–H stretching vibrations are observed in the region between 2800 cm^{-1} and 3200 cm^{-1}. In particular, the band appearing in the Raman spectrum close to 3000 cm^{-1} is assigned as an almost pure band, i.e., as the stretching vibration of N4-H unit, while the bands observed between 2749 and 2886 cm^{-1} are assigned as stretching vibrations of C–H. Stretching vibrations related to C–H of the R1 ring are observed at 3060 and 3130 cm^{-1}; obviously, no stretching associated to R2 ring are observed in the region of 3000 cm^{-1}, because in such a ring the carbon atoms are not bonded to any hydrogen atom. The FT-IR spectrum from the crystal showed two bands above this region, namely at 3241 cm^{-1} (ω_{cal} = 3721 cm^{-1}) and 3385 cm^{-1} (ω_{cal} = 3872 cm^{-1}), corresponding to the symmetric stretching and asymmetric stretching of water, respectively. This corroborates the fact that the crystal under study contains water. Finally, it is important to point out that in the Table 2 there is no assignment to external modes. In fact, the calculation was performed in a isolated molecule $C_9H_{10}N_4O_4{\cdot}H_2O$ what means that it cannot furnish vibrations related to lattice

modes. However, it is well known that such a kind of modes must be found up to 200 cm^{-1} and, consequently, in this region it is expect to be found also, the external modes.

In order to illustrate the assignment, atomic displacement vectors corresponding to two selected normal modes from the isolated molecular structure of $C_9H_{10}N_4O_4{\cdot}H_2O$ are shown in Fig. 4. In Fig. 4a it is shown the representation of the atomic vibrations giving rising to the band observed at ~220 cm^{-1}, which corresponds mainly to the torsional vibration of the two CH_3 groups bonded to the R2 ring. On the other hand, in Fig. 4b it is shown the representation of the atomic vibrations giving rising to the band observed at ~930 cm^{-1}, which corresponds to vibrations of R1 ring.

5. Conclusions

A study on vibrational properties with an exhaustive frequency assignment of 2,2-dimethyl-5-(4H-1,2,4-triazol-4-ylaminomethylene)-1,3-dioxane-4,6-dione monohydrate, $C_9H_{10}N_4O_4{\cdot}H_2O$, was performed using the FT-IR and FT-Raman data as well as DFT calculations. The correlation between calculated and experimental values was very good, and for the first time the Potential Energy Distribution (PED) is being presented for this synthetic substance. Due to the size of the molecule, and the numerous superposition of vibrational modes, bands assignment would have turned impossible without help from the theoretical model, making a clear statement that theory and experiment must go together.

Acknowledgments

We thank CENAPAD-SP for the use of the GAUSSIAN 03 software package and for computational facilities made available through the Project "proj373". Financial support from FUNCAP and CNPq is also acknowledged.

Appendix A. Supplementary material

Supplementary data associated with this article can be found, in the online version, at http://dx.doi.org/10.1016/j.molstruc.2012.12.058.

References

[1] S.M. Desenko, Chem. Heterocycl. Comput. (1995) 2–24.
[2] A.K. Gupta, K.P. Bhargava, Pharmazie 33 (1978) 430–431.
[3] D.H. Jones, R. Slack, S. Squires, K.R.H. Wooldridge, J. Med. Chem. 8 (1965) 676–680.
[4] J.K. Sughen, T. Yoloye, Pharm. Acta Helv. 58 (1978) 64–68.
[5] A. Cansiz, J. Chem. Soc. Pak. 23 (2001) 237–240.
[6] J.M. Kane, M.W. Dudley, S.M. Sorensen, F.P. Miller, J. Med. Chem. 31 (1988) 1253–1258.
[7] S. Massa, R. Disanto, A. Retico, M. Artico, N. Simonetti, G. Fabrizi, D. Lamba, Eur. J. Med. Chem. 27 (1992) 495–502.
[8] A.E.-A.M. Gaber, H. McNAB, Synthesis 14 (2001) 2059–2074.
[9] A.S. Ivanov, Chem. Soc. Rev. 37 (2008) 789–811.
[10] INC. Sterling Drug, Aromatic Amine Derivatives and Preparation. Patent, 464850, 1965. Chem. Abstract 1,147,759, 1966.
[11] L.E. Silva, G.I. Graf, D. Hastreiter, L.E. da Silva, R.A. Rebelo, A.G. Montalbanb, A. McKillop, Tetrahedron 58 (2002) 9095–9100.
[12] P.G. Baraldi, M.G. Pavani, M.C. Nuñez, P. Brigidi, B. Vitali, R. Gambaric, R. Romagnolia, Bioorg. Med. Chem. 10 (2002) 449–456.
[13] A.C. Joussef, L.E. Silva, A.J. Bortoluzzi, S. Foro, Acta Cryst. E 61 (2005) O2642–O2643.
[14] M.J. Frisch, G.W. Trucks, H.B. Schlegel, G.E. Scuseria, M.A. Robb, J.R. Cheeseman, J.A. Montgomery, Jr., T. Vreven, K.N. Kudin, J.C. Burant, J.M. Millam, S.S. Iyengar, J. Tomasi, V. Barone, B. Mennucci, M. Cossi, G. Scalmani, N. Rega, G.A. Petersson, H. Nakatsuji, M. Hada, M. Ehara, K. Toyota, R. Fukuda, J. Hasegawa, M. Ishida, T. Nakajima, Y. Honda, O. Kitao, H. Nakai, M. Klene, X. Li, J.E. Knox, H.P. Hratchian, J.B. Cross, C. Adamo, J. Jaramillo, R. Gomperts, R. E. Stratmann, O. Yazyev, A.J. Austin, R. Cammi, C. Pomelli, J.W. Ochterski, P.Y. Ayala, K. Morokuma, G.A. Voth, P. Salvador, J.J. Dannenberg, V.G. Zakrzewski, S. Dapprich, A.D. Daniels, M.C. Strain, O. Farkas, D.K. Malick, A.D. Rabuck, K. Raghavachari, J.B. Foresman, J.V. Ortiz, Q. Cui, A.G. Baboul, S. Clifford, J. Cioslowski, B.B. Stefanov, G. Liu, A. Liashenko, P. Piskorz, I. Komaromi, R.L. Martin, D.J. Fox, T. Keith, M.A. Al-Laham, C.Y. Peng, A. Nanayakkara, M. Challacombe, P.M.W. Gill, B. Johnson, W. Chen, M.W. Wong, C. Gonzalez, J.A. Pople, Gaussian 03, Revision B.02, Gaussian, Inc., Pittsburgh, PA, 2003.
[15] C.T. Lee, W.T. Yang, R.G. Parr, Phys. Rev. B 37 (1988) 785–789.
[16] R.G. Parr, W. Yang, Density Functional Theory of Atoms and Molecules, Oxford University Press, New York, 1989.
[17] A.D. Becke, J. Chem. Phys. 98 (1993) 5648–5652.
[18] J.M.L. Martin, C. Van Alsenoy, GAR2PED, A Computer Program for PED Calculations, University of Antwerp, Belgium, 2007.
[19] P. Pulay, G. Fogarasi, F. Pang, J.E. Boggs, J. Am. Chem. Soc. 101 (1979) 2550–2560.
[20] G. Fogarasi, X. Zhou, P.W. Taylor, P. Pulay, J. Am. Chem. Soc. 114 (1992) 8191–8201.
[21] A. Kucsman, I. Kapovits, Nonbonded sulfur–oxygen interaction in organic sulfur compounds, In: F. Bernardi, I.G. Csizmadia, A. Mangini (Eds.), Organic Sulfur Chemistry: Theoretical and Experimental Advances, Elsevier, Amsterdam, 1985, pp. 191–245.
[22] P. Veerapandian (Ed.), Structure-based Drug Design, Marcel Dekker, New York, 1997.
[23] P.J. Goodford, in: C. Silipo, A. Vittoria (Eds.), QSAR: Rational Approaches to the Design of Bioactive Compounds (Pharmacochemistry Library, vol. 16), Elsevier Sciences Pub., Amsterdam, 1990, pp. 49–55.
[24] G.R. Desiraju, T. Steiner, 'Structural Chemistry and Biology', International Union of Crystallography Monographs on Crystallography, vol. 9, Oxford University Press, Oxford, 1999.
[25] V. Rajnikant, J. Dinesh, C. Bhavnaish, J. Chem. Cryst. 38 (2008) 567.
[26] M.W. Wong, Chem. Phys. Lett. 256 (1996) 391–399.
[27] A.P. Scott, L. Radom, J. Phys. Chem. 100 (1996) 16502–16513.